MAGNETIC CONJUGACY AS OBSERVED AT THE APEX OF FIELD LINES: GEOS-1 AND -2 RESULTS

Roger Gendrin

Centre de Recherches en Physique de l'Environnement, Centre National d'Etudes des Télécommunications, 92131 Issy-les-Moulineaux, France

Abstract: This report is the written version of an invited review presented at the Nagata Symposium on Geomagnetically Conjugate Studies which was held during the 19th SCAR General Assembly. It deals with the relationships which exist between phenomena occurring at the apex of field lines, as detected by the European spacecraft GEOS-1 and -2, and those occurring at their foot prints, as observed by ground-based, balloons and rockets (GBR) techniques. Such simultaneous observations have allowed to obtain a more quantitative description of already known phenomena and to discover some new ones. The following topics are discussed in the paper: generation and propagation characteristics of ion cyclotron waves (ICW) in multi-component plasmas, quasi-linear interaction between VLF hiss and energetic electrons, cold plasma behaviour in the equatorial plasmasphere and its relationship with the global magnetospheric convection, existence of small-scale intense field-aligned currents (FAC).

1. Introduction

The Earth magnetic lines of force play an ordering role in almost all magnetospheric processes whether they involve waves or particles. Ground-based, Balloon or Rocket (GBR) experiments (whether passive or active) performed in conjugate areas have contributed a lot in demonstrating this role. The advantage of complementing these experiments by measurements at a third point situated near the apex of the field line is two-fold:

1) A reasonably well equipped spacecraft can provide direct information on parameters which can be only indirectly inferred from GBR measurements. Among those, the values of the DC electric field intensity and direction, and of the cold plasma density, or the pitch angle distribution of energetic particles, are key parameters which can be obtained, with reasonable confidence, only by direct *in situ* measurements.

2) A lot of phenomena, which occur at the apex of field lines, are not detectable on the ground or even at ionospheric altitudes. The survey of such phenomena is mandatory if one wants to have a precise evaluation of the energy transfer between the solar wind, the magnetosphere and the ionosphere-thermosphere system, since a non negligible part of these transfer processes could escape from GBR measurements alone.

Moreover, when situated at a geostationary position (the only position where continuous measurements can be done in conjugate areas), a spacecraft will lie in the region where most of large scale magnetospheric phenomena are initiated. The $L=$

6.6 position is at the boundary between the plasmasphere and the plasmasheet. It lies on auroral field lines, and it may even sometimes cross the magnetopause.

Having these considerations in mind, the European Space Agency (ESA) and the European Scientific Community decided to built the first fully scientific geostationary spacecraft, GEOS. A full description of the GEOS spacecraft equipments can be found in KNOTT (1975). Detailed reports on the wave and plasma experiments, which are of our main concern here, have been published by JONES (1978) and S-300 EXPERIMENTERS (1979).

Because of a failure in the launching process, the first spacecraft GEOS-1 (launched in April 1977) did not reach its geostationary position. However it gave a lot of information on the radial variation of different parameters and it validated the new techniques which had been implemented for measuring the DC electric field, the cold plasma density or composition (see KNOTT *et al.*, 1979). GEOS-1 was not permanently conjugated with ground stations. However the foot prints of the magnetic lines of force passing through it encircled two points in the northern and southern hemisphere (Husafell in Iceland, and Syowa Station in Antarctica) where observations of ULF and VLF emissions, auroral luminosity and ionospheric absorption were conducted (Fig. 1). The results thus obtained have helped to understand the generation and propagation characteristics of different electromagnetic waves (CORNILLEAU-WEHRLIN *et al.*, 1978a; GENDRIN *et al.*, 1978; PERRAUT *et al.*, 1984; YAMAGISHI *et al.*, 1984; TIXIER and CORNILLEAU-WEHRLIN, 1986).
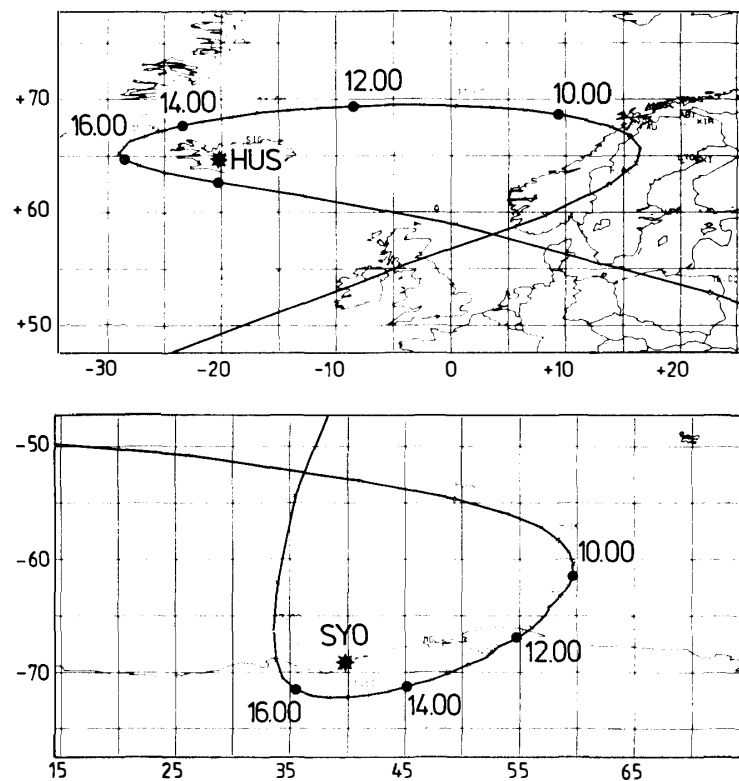

Fig. 1. Foot print of the magnetic field lines passing through GEOS-1 in July 1977. Husafell (HUS) and Syowa Station (SYO) are the two stations were simultaneous ground observations were performed (courtesy by J. C. KOSIK).
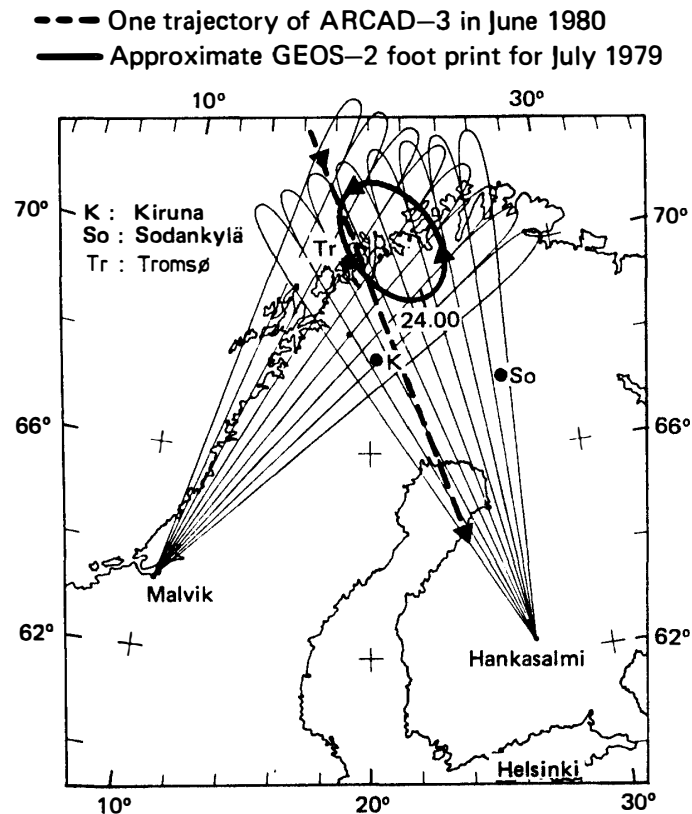
Fig. 2. Map of Northern Scandinavia showing the experimental facilities which could be used in conjunction with GEOS-2. Original map by GREENWALD et al. (1978), showing the STARE radars field of view. Situation of the three EISCAT stations: Tromsø, Kiruna and Sodankylä. Foot print of GEOS-2 when situated at 35° east longitude (quiet magnetic conditions). An example of the trace of the French-Soviet ARCAD-3 satellite in January 1981.

GEOS-2 (launched in July 1978) was a truly geostationary satellite. Its longitude could be changed between 5° and 37° east in order to allow conjugated studies in different areas as well as the study of the equatorial confinement of some electrostatic emissions (i.e. CHRISTIANSEN et al., 1980; GOUGH et al., 1981; CANU, 1982). However most of the time GEOS-2 was situated at 35° east, a longitude which gives the best conjugacy with the Scandinavian auroral zone. Figure 2 shows the trace of the foot print of the field line passing through GEOS when situated at such a longitude, the small diurnal variation being due to the assymetry of the Earth magnetic field. Also represented on Fig. 2 are the positions of the three stations of the EISCAT ionospheric incoherent sounder and the traces of the STARE radar beams. A line representing the projection of the French-Soviet ARCAD-3 trajectory during one of its pass is also represented. These equipments were complemented by optical instruments (SHEPHERD et al., 1980), by magnetometer chains (KÜPPERS et al., 1979), by the STARE radar system (GREENWALD et al., 1978) or by balloon campaigns (KREMSER et al., 1986), all of these operating in conjunction with GEOS-2.

Such a combination of facilities explains the importance of the harvest of data thus obtained. In what follows we will discuss those data by which the exact degree of conjugacy between GBR observations and observations made at the apex of the

Table 1.   List of GEOS-associated GBR experiments discussed in the text.

Place of experiment	Year	Studies topic	Section
GEOS-1			
Husafell (Iceland) and Syowa (Antarctica)	1977	ULF, VLF generation and propagation	2. 1, 3. 3
GEOS-2			
Kilpisjärvi (Finland)	1978	Optical emissions	5. 1
Scandinavian and Canadian magnetometer chain	1979	Long period ULF pulsations	2. 4
Balloons (Scandinavia)	1979	Wave particle interactions	3. 1
Kitdalen, Skibotn (Norway) and Syowa (Antarctica)	1980–81–82	ULF, VLF generation and propagation	2. 1, 2. 3, 3. 3
STARE	1978	Long period ULF pulsations	2. 4
	1978–79	Plasma convection	4. 3
EISCAT	1982	Wave-particle interactions	3. 2
	1982	Plasma convection	4. 3
ARCAD	1982	Particle precipitation	3. 2
	1982	Field-aligned currents	5. 3

field line can be established (see Table 1).   We will deal successively with wave generation and propagation mechanisms (in both ULF and VLF ranges), cold plasma density and magnetospheric convection, field-aligned current structures.

2.   ULF Waves

The very first results obtained with GEOS showed that the classification of ULF waves which had been established on the basis of a long series of ground observations (*i.e.* GENDRIN, 1970) was not exactly valid in space.

For instance repetitive structures, which correspond to "pearl oscillations" and from which propagation time between the equatorial plane and the ground could be measured, were observed only with GEOS-1 for *L*-values smaller than 5 (PERRAUT *et al.*, 1978; GENDRIN *et al.*, 1978).   Similarly IPDP's were not observed in space, as one could expect, since the frequency change of such events corresponds to inward and azimuthal displacement of the source region, which cannot be followed by a geostationary satellite.

But two new kinds of ULF electromagnetic signals were observed.   Their frequency-time structures are depicted on Fig. 3.

2.1.   Ion cyclotron waves (ICW) in multicomponent plasmas

The first kind corresponds to waves which propagate parallel to the DC magnetic field, B_0.   It consists of two emissions generated in two frequency bands, one below and one above the local He^+ gyrofrequency (Fig. 4).   A systematic study of the conjugacy relationships which exist for these emissions has shown that the low frequency signal is always detected at ground, as opposed to less than half of the high frequency signals (PERRAUT *et al.*, 1984).   Figure 5 illustrates such an observation, which agrees with the theoretical study of ICW's propagation in a plasma containing a non negligible amount of cold He^+ ions (RAUCH and ROUX, 1982).   This study shows that, because of the variation of the plasma characteristic frequencies along a given field
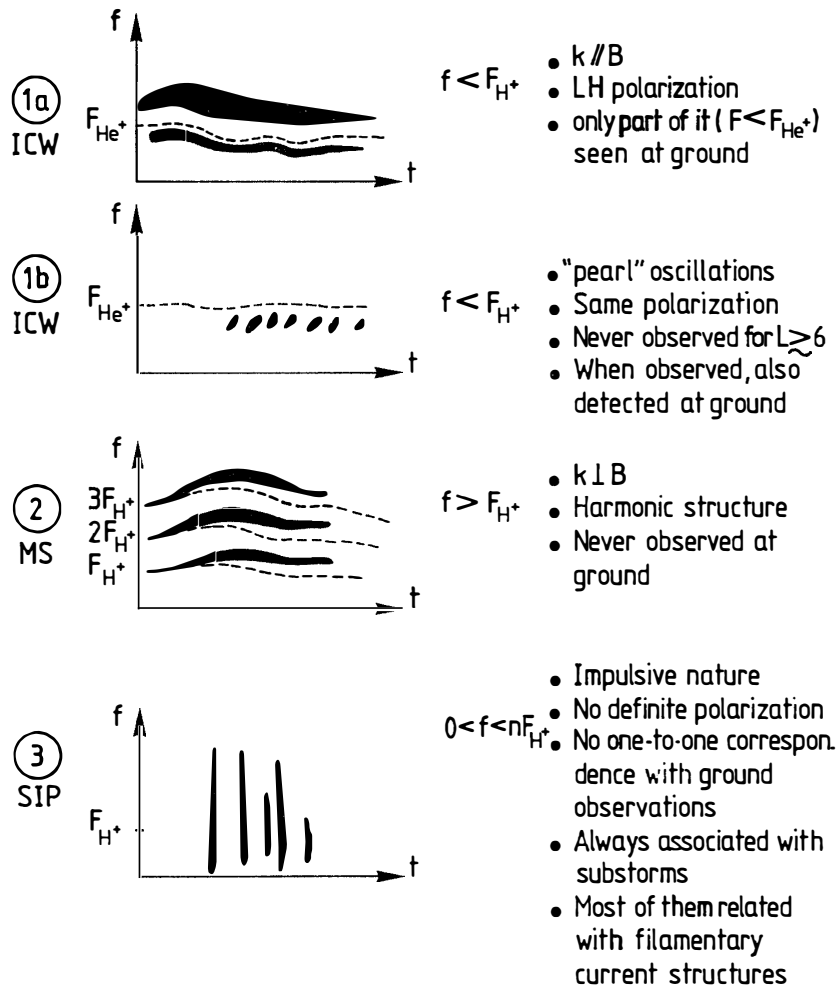
Fig. 3. Schematic spectrograms of ULF waves detected onboard GEOS: 1) Ion cyclotron waves, 2) Magnetosonic waves, 3) Short irregular pulsations.

line, only waves generated in the left-handed (LH) mode below the equatorial He$^+$ gyrofrequency will systematically propagate towards the ground (Fig. 6). Waves generated above the equatorial cut-off frequency and below the equatorial cross-over frequency will be deflected towards the outer magnetosphere. Waves generated above the cross-over frequency will be confined near the equatorial region and will be reflected at the point where their frequency is equal to the local bi-ion frequency. However a tunnelling effect, whose efficiency depends upon both the wave frequency and the He$^+$ concentration ratio, allows the transmission to the ground of a fraction of the power generated in this mode, as observed (PERRAUT *et al.*, 1984).

These observations have emphasized the prominent role of the presence of cold He$^+$ ions in the propagation and generation of ICW's. They have stimulated a lot of observational works as well as numerical simulation studies on the origin and consequences of ICW's in multicomponent plasmas. These consequences are two-fold: 1) the heating of He$^+$ ions to suprathermal energies, mainly in the direction perpendicular to the DC magnetic field (GENDRIN and ROUX, 1980; YOUNG *et al.*, 1981; GENDRIN, 1981, 1983; ROUX *et al.*, 1982; GENDRIN *et al.*, 1984; OMURA *et al.*, 1985;
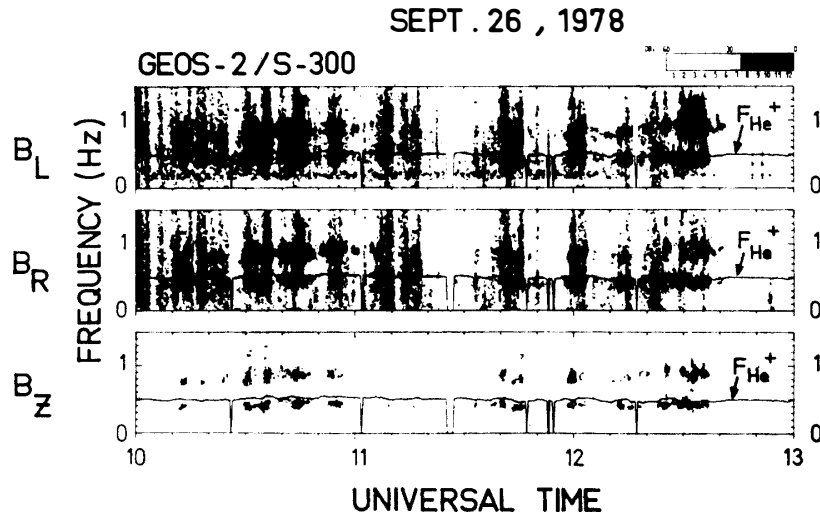
SEPT . 26 , 1978

Fig. 4. Example of an ion cyclotron wave event. The emission takes place in two frequency bands. The continuous line corresponds to the He$^+$ gyrofrequency as deduced from the DC magnetometer. The two upper panels correspond to LH and RH polarized signals in a direction perpendicular to the spin axis (i.e. almost perpendicular to the DC magnetic field, B_0) The low intensity of the signal in the direction parallel to the spin axis (the lowest panel) indicates that the signal mainly propagates in a direction parallel to B_0 (ROUX et al., 1982).
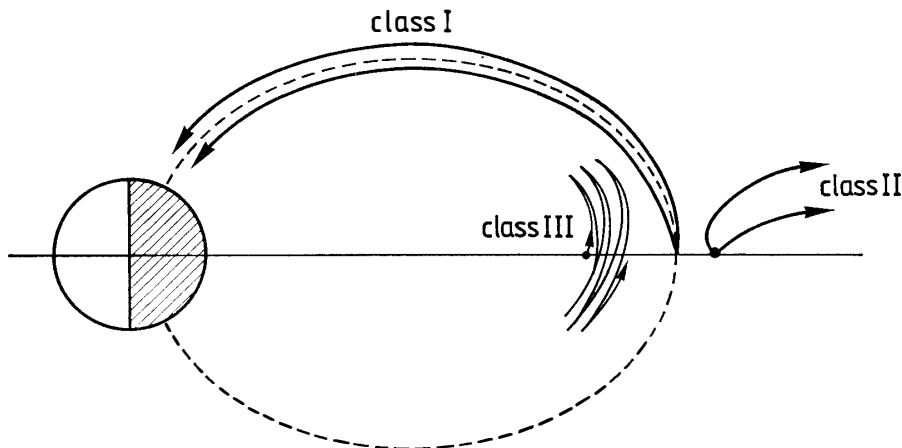

Fig. 5. Result of ray tracing computations for ion cyclotron waves generated in the LH mode in a He$^+$ rich plasma. Waves are classified according to the relative value of their frequency with respect to the equatorial characteristic frequencies of the medium: class I: $f<F_{He^+}$ (those waves can reach the ground); class II: $F_{co}<f<F_{cr}$, where F_{co} is the cut-off frequency and F_{cr} the cross-over frequency (those waves never reach the ground); class III: $f>F_{cr}$ (those waves are reflected at the place where $f=F_{bi}$, the local bi-ion hybrid frequency). By a tunnelling mechanism a fraction of these waves can reach the ground (after RAUCH and ROUX, 1982).

BERCHEM and GENDRIN, 1985); 2) the parallel acceleration of thermal electrons (COR-NILLEAU-WEHRLIN, 1981; NORRIS et al., 1983; ROUX et al., 1984).

2.2. Magnetosonic waves

The second kind of ULF electromagnetic waves which were discovered in space are magnetosonic (MS) waves. They propagate in a direction almost perpendicular
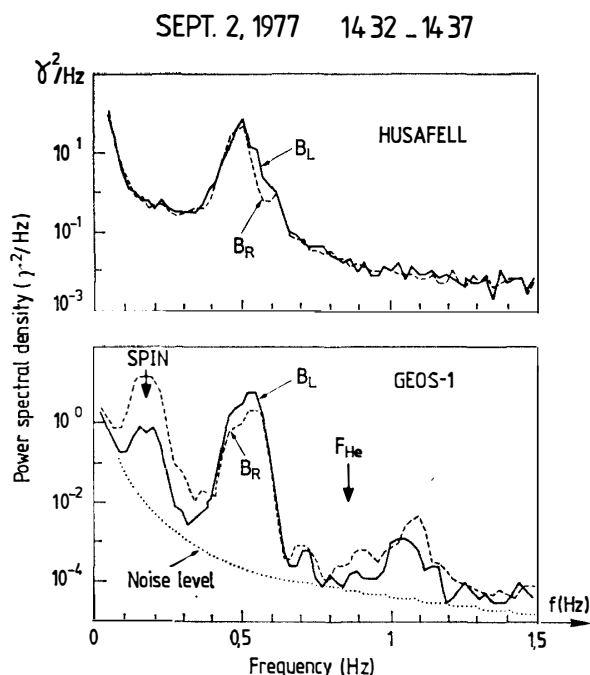
Fig. 6.   Spectra of ICW's detected simultaneously onboard GEOS and at ground.   Only the low
frequency part of the signal is detected at Husafell.   Because of the rather high magnetic
latitude of GEOS-1 at that time ($\sim30°$), the high frequency part of the emission is almost
linearly polarized.   The signal at the spin frequency is induced by the rotation of the spacecraft
(PERRAUT et al., 1984).

to the DC magnetic field and they have a multiharmonic structure (see Fig. 3, third panel).   These waves, whose origin lies in the existence of ring distributions in the velocity space or of spatial gradients in the energetic proton population (PERRAUT et al., 1982; KORTH et al., 1983) are never detected on the ground.   Their consequences on the dynamics of energetic particles or on cold plasma heating are not yet completely elucidated.

2.3.   Short irregular pulsations

Short irregular pulsations (SIP) are often observed on board GEOS (see Fig. 3, lower panel).   Their spectra may extend to rather high frequencies (i.e. 11 Hz, which is the maximum frequency detectable on the GEOS ULF magnetic sensors).   They are observed mainly during magnetospheric substorms (see Section 5.1).   Similar emissions are detected at ground, also during substorm conditions, but their maximum frequency rarely exceeds 5 Hz.   A systematic search of simultaneity between space and ground (including possible propagation delays) has shown that no one-to-one correspondence could be established for the individual pulses.   The nature of these signals as well as the reasons for the absence of precise conjugacy relationships will be discussed in Section 5.

2.4.   Other ULF signals

Emissions at lower frequencies have been also detected onboard GEOS.   These emissions have been studied by using GEOS electric and magnetic data alone (JUN-

GINGER *et al.*, 1983, 1984), or in conjunction with other equipments like onboard particle detectors (KREMSER *et al.*, 1981), ground magnetometer stations (WEDEKEN *et al.*, 1984), or the STARE radar system (WALKER *et al.*, 1982). The conclusions of these studies are that, in the Pc 4–5 frequency range, all known excitation mechanisms (Kelvin-Helmholtz or drift-mirror instabilities, associated or not with field line resonance) can be at their origin. Besides, O^+ ions seem to play a role in the generation of some Pc-2 emissions (INHESTER *et al.*, 1984; WEDEKEN *et al.*, 1984).

3. VLF Waves

The study of VLF waves onboard GEOS took advantage of the following capabilities: 1) a large frequency coverage (0–77 kHz), extending well above the local plasma frequency f_{pe}, for most of the time and up to ~ 30 harmonics of the electron gyrofrequency f_{ce}; 2) a good frequency resolution (down to 10 Hz in the swept frequency mode), 3) measurement of both magnetic and electric components, giving the possibility to distinguish between electromagnetic and electrostatic emissions; 4) measurement of three magnetic components allowing to determine the wave normal direction for electromagnetic modes; 5) regular and reliable measurement of the cold plasma density.

In a review which is devoted to conjugacy aspects of wave or particle phenomena, there is no room to report on all the results which have been obtained by using such facilities. In particular those results which concern natural emissions at the characteristic frequencies f_{pe}, f_{uh}, f_q, emissions at $(n+1/2) f_{ce}$, auroral kilometric radiation or thermal continuum emission will not be reported: the first two categories of emissions, which are purely electrostatic, are more or less localized in space and they do not propagate over long distances; the last two kinds of emissions are electromagnetic but their frequency is such that they cannot propagate in regions of high plasma density, so that they cannot reach the ground.

We will concentrate here on VLF emissions which propagate in the whistler mode, *i.e.* whose frequency in the generation region is smaller than the local electron gyrofrequency. In this frequency range, conjugated studies performed with ground or balloon equipments have led to a quantitative verification of the quasi-linear theory of generation of VLF hiss (Section 3.1). The respective roles of electromagnetic (VLF hiss) and electrostatic ($(n+1/2) f_{ce}$) emissions in precipitating electrons have also been established (Section 3.2). Finally, a detailed analysis of ground and satellite magnetometer data has shed a new light on the origin of VLF quasi-periodic (QP) emissions (Section 3.3). Results obtained by studying the propagation of artificial VLF signals induced by powerful ground transmitters can be found elsewhere in the literature (CORNILLEAU-WEHRLIN *et al.*, 1978c; UNGSTRUP *et al.*, 1978; NEUBERT *et al.*, 1983).

3.1.   Verification of the quasi-linear theory of VLF hiss generation

The self-consistent theory of VLF emission and particle diffusion through a gyroresonant interaction between waves and energetic and anisotropic electrons (KENNEL and PETSCHEK, 1966; ETCHETO *et al.*, 1973) predicts that the wave power, $b_f{}^2$ should depend on three factors: the cold plasma density n_0, the number of resonant electrons
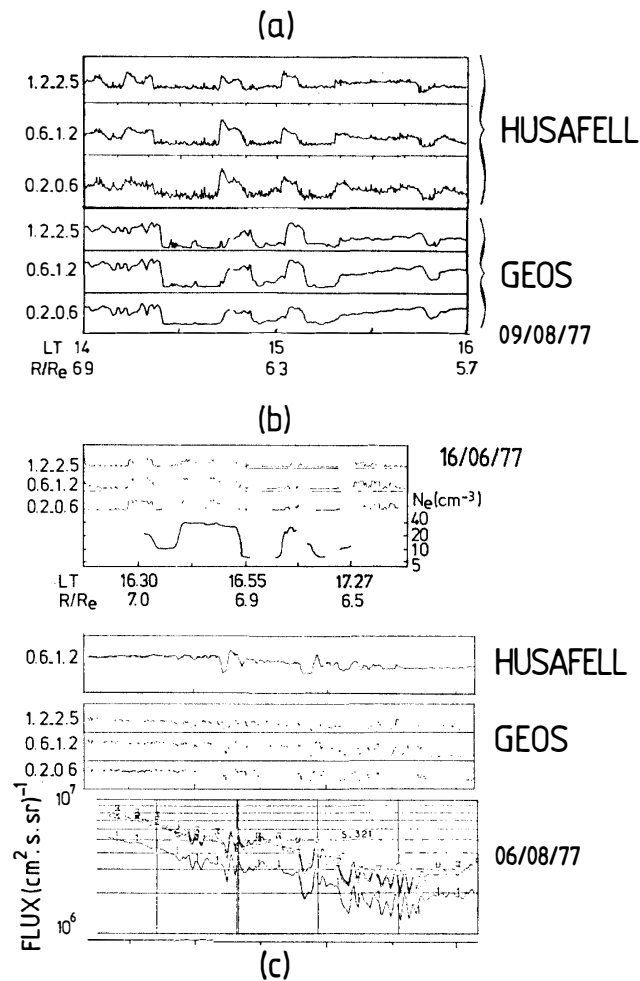
Fig. 7.   VLF emissions observed in the same frequency channels (in kHz) at Husafell and onboard
         GEOS.   (a) Identity of the wave intensities.   (b) The wave intensity is stronger when the
         equatorial cold plasma density is larger.   (c) Fluctuations in the wave intensity also depend
         on the energetic electron flux (after CORNILLEAU-WEHRLIN et al., 1978a, b).

η (E_r) where E_r is the parallel resonant energy corresponding to the generated frequency
f, and the anisotropy A (E_r) of the electron distribution at this parallel energy.

Preliminary observations made at Husafell in conjunction with GEOS-1 has
given a qualitative confirmation of the role played by the two first parameters.   Figure
7, which is a combination of results thus obtained (CORNILLEAU-WEHRLIN et al., 1978a,
b), shows that: 1) VLF signals are detected simultaneously at the ground and onboard
the spacecraft when the conjugacy relationship is good and when there is no strong
ionospheric absorption induced by intense electron precipitation; 2) the wave intensity
is stronger when the equatorial cold plasma density is larger; 3) the wave intensity is
also closely related with the electron flux.

The role of the third parameter, A has been demonstrated through a detailed
analysis of the GEOS energetic particle data, (CORNILLEAU-WEHRLIN et al., 1985)
which has allowed the precise computation of both η (E_r) and A (E_r) and therefore
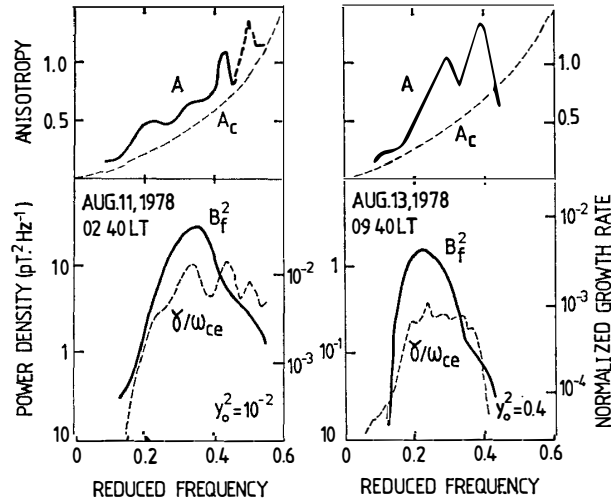of the growth rate γ (f).   This analysis, shows that: 1) the spectral structure of the

Fig. 8. Comparison between the measured wave power B_f^2 (as a function of the reduced frequency f/f_{ce}) and the computed normalized growth rate $\gamma/2\pi f_{ce}$, as deduced from the electron distribution function. The anisotropy A (f) which is also deduced from the electron distribution function is larger than the critical anisotropy in the frequency range of the emission. In weak diffusion (weak field, right pannel), A is much larger than A_c. In strong diffusion (left pannel), A approaches the critical anisotropy (after CORNILLEAU-WEHRLIN et al., 1985).
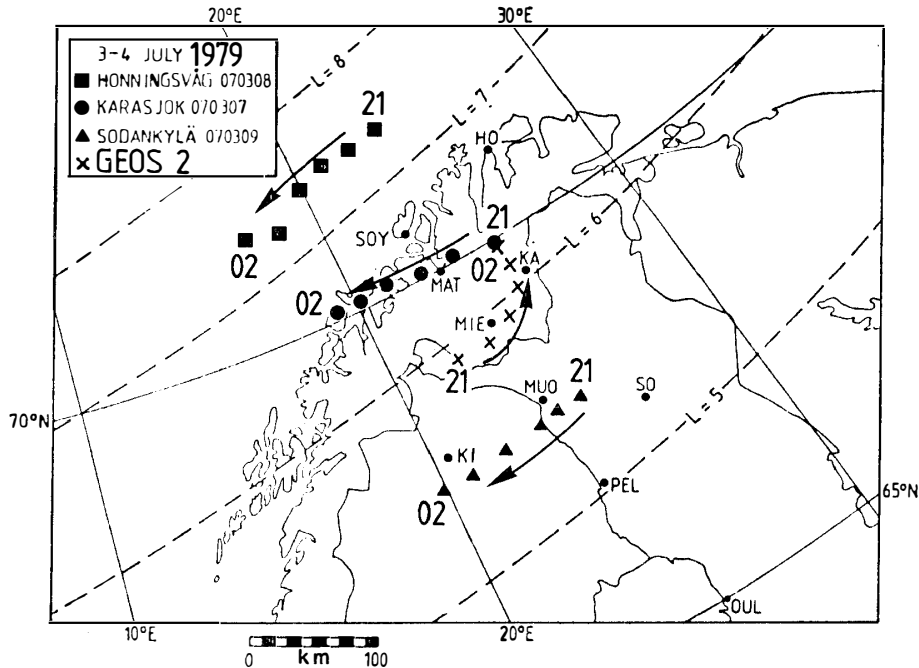

Fig. 9. Trajectories of balloons launched from three Scandinavian stations: Honningsvåg, Karasjok and Sodankylä. Also plotted is the nominal foot print (×) of GEOS-2 field lines between 21 and 02 UT (KREMSER et al., 1986).

observed wave power is identical to the spectral structure of the computed growth rate; 2) the observed anisotropy is larger than the critical anisotropy $A_c = (f_{ce}/f - 1)^{-1}$ in the whole frequency range of the emission; 3) the difference $A - A_c$ is smaller when the wave intensity is larger (Fig. 8). These conclusions agree with the quasi-linear

theory which implies that when the wave amplitude is large the diffusion is strong and the anisotropy decreases until a situation where waves are no more generated is reached.   Henceforth the tendency, in the case of strong diffusion, for the curve A (f) to follow the curve A_c (f).
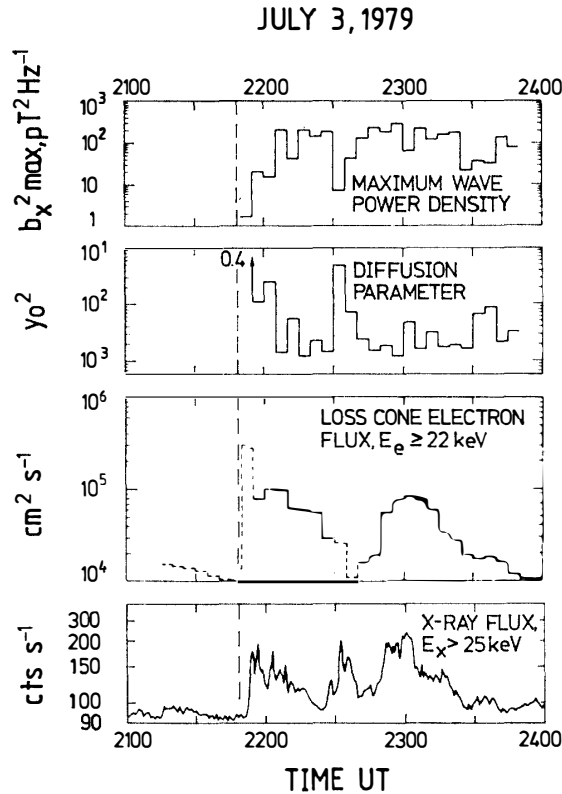

Fig. 10.   Comparison between observed wave intensity, computed diffusion parameter, measured loss-cone electron flux (at the geostationary orbit) and X-ray flux detected onboard a balloon launched in the conjugate region (KREMSER et al., 1986).

An attempt to check these conclusions until their final consequence, *i.e.* the increase of particle precipitation when the diffusion strength becomes large has been made by combining the wave spectrum and electron distribution function measured on board GEOS-2 with X ray fluxes measured onboard balloons launched in the conjugate area (KREMSER *et al.*, 1986).   The trajectory of the balloons is represented on Fig. 9 together with the nominal conjugate points of geomagnetic field lines through GEOS-2.   The bottom pannel of Fig. 10 shows the X ray flux ($E > 25$ keV) recorded on the balloon whose trajectory was nearest to the GEOS-2 conjugate points.   Apart from the period between 2230 and 2240, increases in the X ray flux coincide with increase in the loss cone electron flux (third pannel from the top) and in the VLF wave intensity (first pannel), both being measured onboard GEOS.   The diffusion parameter $y_o^2 = \alpha_o^2/DT_e$, where α_o is the half loss cone angle, D the diffusion coefficient (proportional to b_f^2) and T_e the quarter bounce period of the interacting electrons, is also plotted (second pannel).   This pannel shows that when y_o^2 is small (*i.e.* when the diffusion is strong) the flux within the loss cone is large, as is the X ray flux detected at the foot of the field line.

These results confirm the validity of the self-consistent quasi-linear theory of VLF generation by gyroresonant interaction with energetic ($\sim$20 keV) electrons. They also show that most of the energetic electron precipitation can be explained by such an interaction.

3.2. The respective role of electromagnetic and electrostatic waves in particle precipitation

Another candidate for interpreting continuous patricle precipitation in the aurora region is the electrostatic emissions which often occur around half-integer harmonics of the electron gyrofrequency (KENNEL et al., 1970; LYONS, 1974; ASHOUR-ABDALLA and KENNEL, 1978). However the confinement of this emission in a very small latitude range in the vicinity of the geomagnetic equator (CHRISTIANSEN et al., 1980; GOUGH et al., 1981; CANU, 1982) has been at the origin of a controversy about whether or not these waves had a sufficient energy, integrated along the field line, to be able to precipitate medium energy electron (BELMONT et al., 1983, 1984).

In an attempt to clarify this question a systematic study of particle precipitation as observed at ionospheric altitudes by means of the EISCAT facility and of the ARCAD-3 polar orbiting satellite was undertaken, in conjunction with the measurement of electrostatic waves at the field line apex with GEOS (FONTAINE et al., 1986a).

First the ionospheric conductivity profile in the E region deduced from EISCAT measurements were used to compute, by an inversion method, the spectrum of the precipitated electrons. Comparisons with direct measurements made onboard AR-CAD-3 at an altitude of about 1400 km and with measurements made at the altitude of GEOS shows a good agreement between the three spectra. As far as GEOS is concerned, the agreement is not so good at low energies ($<$3 keV) because of the existence, at ionospheric altitudes, of backscattered electrons (Fig. 11).
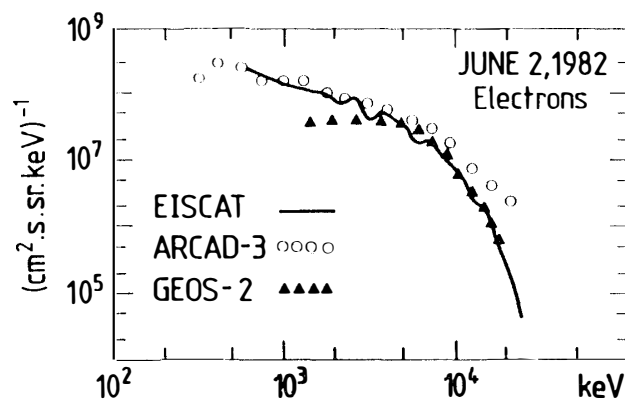

Fig. 11. Electron spectra observed on the Tromso auroral field line June 2, 1982 around 1900 UT. The continuous curve corresponds to the spectra deduced from EISCAT measurements, dots and crosses to direct measurements made at ionospheric altitudes with ARCAD-3 and at the apex of the field line with GEOS-2, respectively (after FONTAINE et al., 1986a).

Second, the electrostatic wave intensity around the strongest of the $(n+1/2)\ f_{ce}$ emissions (i.e. around $3/2 f_{ce}$) was simultaneously measured by using the electric antennas onboard GEOS. Applying the formulas given by BELMONT et al. (1983), it was possible to compute the minimum intensity which is needed to put electrons at different
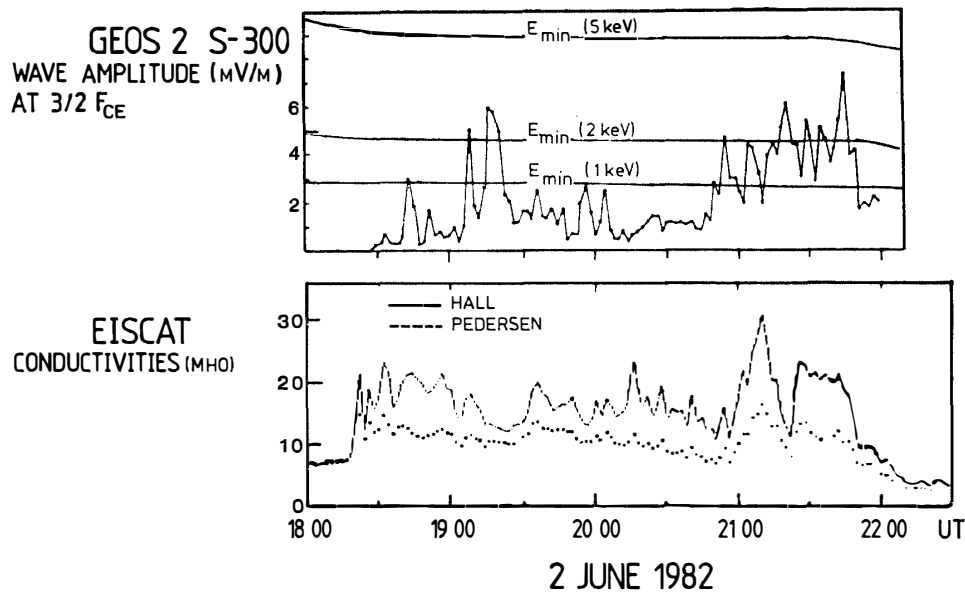
Fig. 12.   Are electrostatic waves around $(n+1/2)f_{ce}$ responsible for electron precipitation in diffuse auroras?   On the lower pannel are represented the ionospheric conductivities as measured with EISCAT.   Increase in these conductivities are indicative of electron precipitation. On the upper pannel the $3/2$ f_{ce} electrostatic wave intensity as observed onboard GEOS-2 is represented, together with the minimum wave intensity required for putting electrons of different energies into strong diffusion (FONTAINE et al., 1986a).

energies in strong pitch angle diffusion, and to compare it with the observed wave intensity.   The results which are shown in Fig. 12 indicate that whereas soft electron precipitation ($E \sim 1$ keV) may be explained by such a mechanism, that is not the case for higher energy electrons.   Some other mechanism has to be sought in order to explain the continuous precipitation of medium energy electrons in diffuse auroras. Electromagnetic cyclotron interaction is a possible candidate, but a systematic study of the corresponding wave intensity in the vicinity of the geostationary altitude has still to be performed.

3.3.   A unified theory of quasi-periodic VLF emissions

Quasi-periodic (QP) VLF emissions are electromagnetic waves which are detected at the ground in the VLF range ($\sim 0.2-3$ kHz) and the amplitude of which is modulated with periodicities ranging from tens of seconds to 2 or 3 min.   These emissions are not to be confused with those having much shorter periodicity (HELLIWELL, 1963; BRICE, 1965; YAMAGISHI et al., 1984).   Classically they are divided into two categories: type I QP emissions which are clearly associated with magnetic pulsations of exactly the same period, and type II QP emissions whose association with magnetic pulsations does not always exist and for which, when such an association exists, the two periodicities are not equal (for reviews, see KITAMURA et al., 1969; KIMURA, 1974; SATO and KOKUBUN, 1980, 1981; SATO and FUKUNISHI, 1981).

Conjugate measurements of magnetic ULF and electromagnetic VLF signals have been performed at Husafell and onboard GEOS-1 in an attempt to clarify the relationships existing between these two signals (TIXIER and CORNILLEAU-WEHRLIN, 1986).
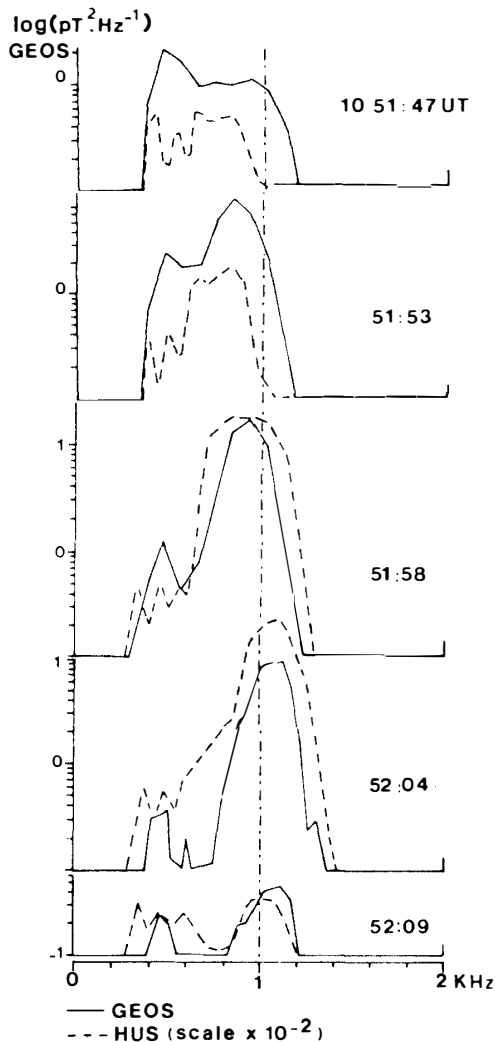
Fig. 13. Identity of VLF wave spectra observed at Husafell and onboard GEOS-1 during a rising tone VLF quasi-periodic emission on August 18, 1977. The power spectral density observed at the ground has been multiplied by 10^2 (TIXIER and CORNILLEAU-WEHRLIN, 1986).
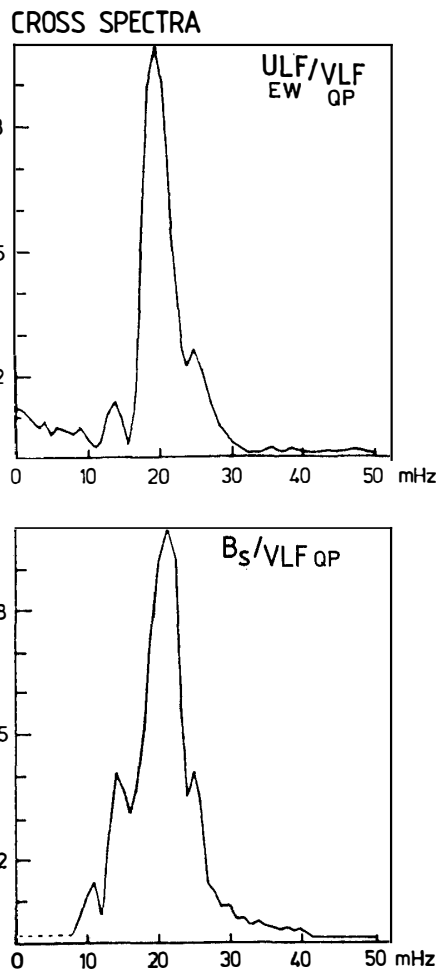
Fig. 14. Cross spectra of the VLF modulation amplitude and the ULF intensity for a type I QP emission (August 20, 1977). Upper pannel: at Husafell; lower pannel: onboard GEOS. In this figure and in the next one, B_a is the intensity of the magnetic field component, measured onboard the spacecraft, in the plane perpendicular to the spin axis (TIXIER and CORNILLEAU-WEHRLIN, 1986).

It must be noted that the geomagnetic latitude of GEOS-1 was varying between $-15°$ and $+30°$ during the observation period. The spectra of the VLF emissions have been found to be identical at the two points of measurements, within a 20 dB attenuation factor (Fig. 13). The comparison between the ULF spectrum and the modulation spectrum of the VLF amplitude (integrated around 900 Hz) has partially confirmed the distinction between the two categories of QP emissions. For type I QP emissions these spectra are identical (Fig. 14). But for type II QP emissions the situation is more complex: 1) the spectra of the VLF modulation and of the ULF waves may contain a number of peaks; 2) these peaks may be different when comparing the GEOS
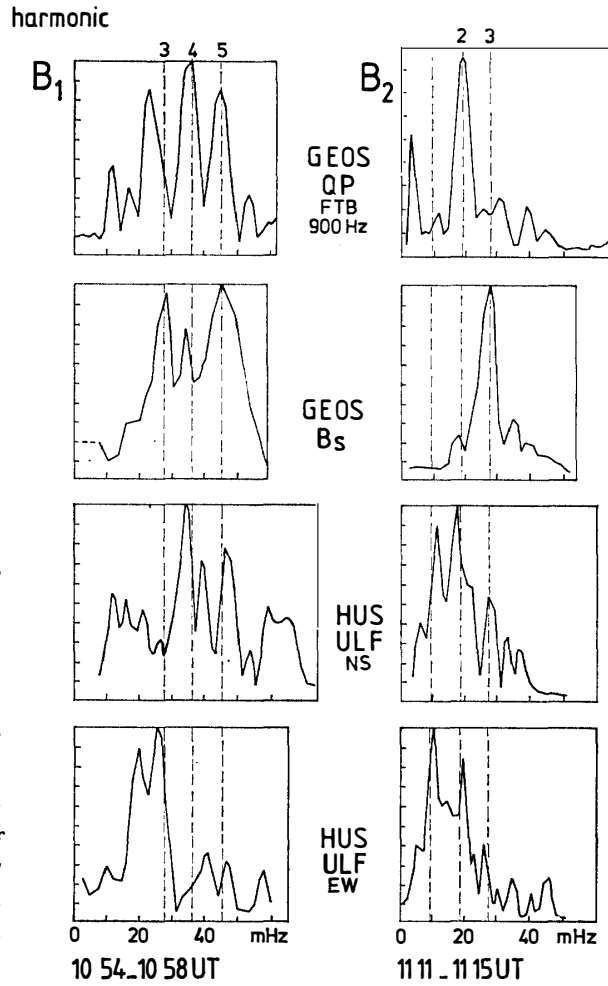
harmonic

Fig. 15. Example of the relationships existing between VLF (type II) QP emissions and simultaneous ULF oscillations (August 18, 1977). From top to bottom: Spectrum of the integrated amplitude of the VLF emission observed onboard GEOS around 900 Hz; Spectrum of the ULF oscillation detected onboard GEOS; Spectrum of the NS component of the ULF oscillation detected at Husafell; Spectrum of the EW component of the ULF oscillation detected at Husafell. All peaks are harmonically related. For the precise definition of B_s see Fig. 14 (TIXIER and CORNILLEAU-WEHRLIN, 1986).
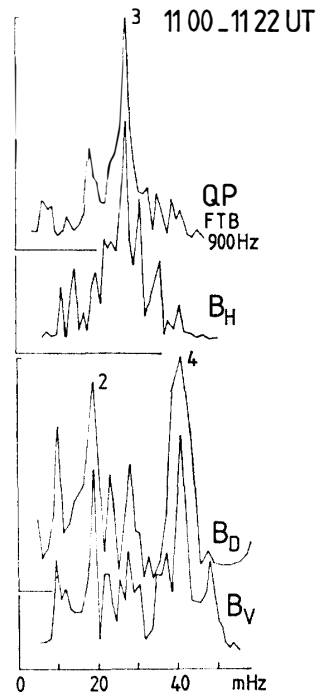
Fig. 16. Spectra of the VLF modulated amplitude and of the three components of the ULF oscillations detected onboard GEOS-2, on February 2, 1980. H: parallel to the spacecraft spin axis (i.e. almost parallel to the DC magnetic field), D: eastward and V vertical. All peaks are harmonically related but the modulation frequency of the VLF amplitude is determined by the frequency of the compressionnal component of the ULF wave (TIXIER and CORNIL-LEAU-WEHRLIN, 1986).

VLF modulation and ULF wave spectra or when comparing the Husafell EW and NS ULF spectra; 3) all these spectral peaks are harmonically related, the fundamental frequency being of the order of 8 mHz, which is similar to (though larger than) the fundamental field line resonance frequency as reported by different authors for this range of L-values (HUGHES and GRARD, 1984; JUNGINGER et al., 1984; TONEGAWA et al., 1984).

Some of these observations are presented on Fig. 15. Their interpretation is linked to the latitude dependence of Pc 3–4 wave structure along magnetic field-lines: the different harmonics of a fundamental field line resonance frequency have different amplitiudes at different latitudes (TAKAHASHI and McPHERRON, 1982). Similarly the relative amplitudes of EW and NS components detected on the ground much depend on ionospheric conditions (i.e. HUGHES and SOUTHWOOD, 1976). Such phenomena explains why all the observed ULF signals do present spectral peaks which may not coincide, but which are harmonics of a same fundamental frequency.

The second result of TIXIER and CORNILLEAU-WEHRLIN's analysis is that the peak frequency of the VLF modulation spectrum coincides with the peak frequency of the longitudinal (compressional) component of the ULF wave as detected in the generation region (Fig. 16). This seems to confirm the interpretation of CORONITI and KENNEL (1970), according to whom the adiabatic modulation of the electron anisotropy by compressional ULF waves is responsible for the modulated VLF emissions and associated particle precipitation.

4. Cold Plasma Density and Global Magnetospheric Convection

One of the major advantages of GEOS for studying wave particle interactions was the presence of active experiments onboard by which the electron concentration could be measured accurately, even in regions of low plasma density. There were two such experiments: the relaxation sounder (RS) and the mutual impedance (MI) experiment. These experiments are based upon the propagation properties of waves in the vicinity of the plasma characteristic frequencies: $f_{pe}, f_{uh}, nf_{ce}, f_{qn}$. Measurements of these frequencies were obtained every 12 mn at least and sometimes with a higher time resolution (ETCHETO and BLOCH, 1978; HIGEL, 1978; DECREAU et al., 1978a, b). Only RS results will be reported here.

4.1.   The cold plasma density at $L=6.6$

Figure 17 illustrates the kind of plots which can be obtained from these measurements. The plasma density, n_e is plotted as a function of local time over a 24 h period of observation. One notices the rather regular behavior of n_e in the day hours (from $\sim$2 to 10 cm^{-3}), a sharp increase (up to $\sim$70 cm^{-3}) when the plasmaspheric bulge is encountered, and the low ($\sim$0.1 to 1 cm^{-3}) and erratic values during the night hours.

The measurement of the central position of the bulge and of its width has been used, in conjunction with other measurements, to evaluate the convection electric field strength (HIGEL and WU, 1984; SONG and CAUDAL, 1987), its relation with the intensity of the interplanetary magnetic field (WU et al., 1981), the shape of the convection potential (WU et al., 1985), the refilling process of the plasmasphere (SONG et
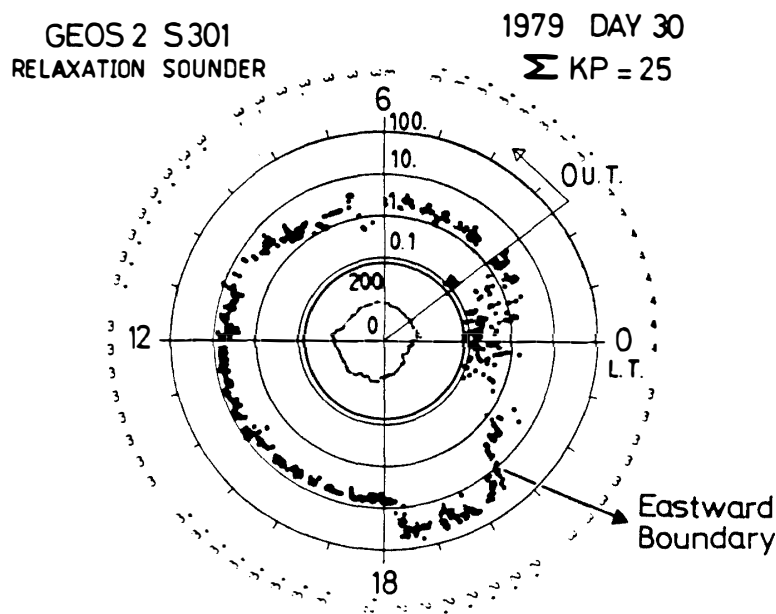
Fig. 17. Plasma density as a function of local time, as deduced from a 24 h period of GEOS-2
measurements.   The plasma density is plotted on a logarithmic scale (from 0.1 to 100 cm⁻³).
The inner curve corresponds to the DC magnetic field intensity (linear scale, from 0 to 200
nT) as deduced from the resonance at the electron gyrofrequency.   The numbers printed
on the outer parts are the Kp indices (after HIGEL and WU, 1984).

al., 1987a); and even to compute the large scale structure of field-aligned currents in
auroral regions (SONG et al., 1987b).

4.2.   The relationship between the plasmaspheric bulge and the Harang discontinuity

What interests us here, because of its relationship with a feature characteristic
of auroral ionosphere, is the eastward border of the bulge region of the plasmasphere
(see Fig. 17), whose local time is denoted by T_P.   As is well known, T_P is a decreasing
function of the geomagnetic planetary index, Kp, the bulge being displaced towards
early hours when the magnetic activity is stronger (i.e. CHEN and WOLF, 1972).   It is
also known that the Harang discontinuity which is observed at ionospheric altitudes
in the auroral zone occurs earlier in the night in similar conditions, i.e. that its local
time, T_H is also a decreasing function of Kp (NIELSEN and GREENWALD, 1979).

In order to establish the possible relationship which could exist between the ob-
served Kp dependence of both T_P and T_H, as systematic study was conducted over a
4-month period (November 1978–March 1979), the purpose of which was to compare
the variation of T_P (as measured through the RS experiment onboard GEOS-2) and
T_H (as measured by using the STARE radar facility) with Kp as well as the relation
between T_P and T_H for individual events.   The results of this study are represented
on Fig. 18, which shows that both T_P and T_H decrease when Kp increases, the variation
of T_H being of a smaller amplitude than that of T_P (ZI et al., 1982).   Such an observa-
tion is interpreted in terms of a rotation and intensification of the global magneto-
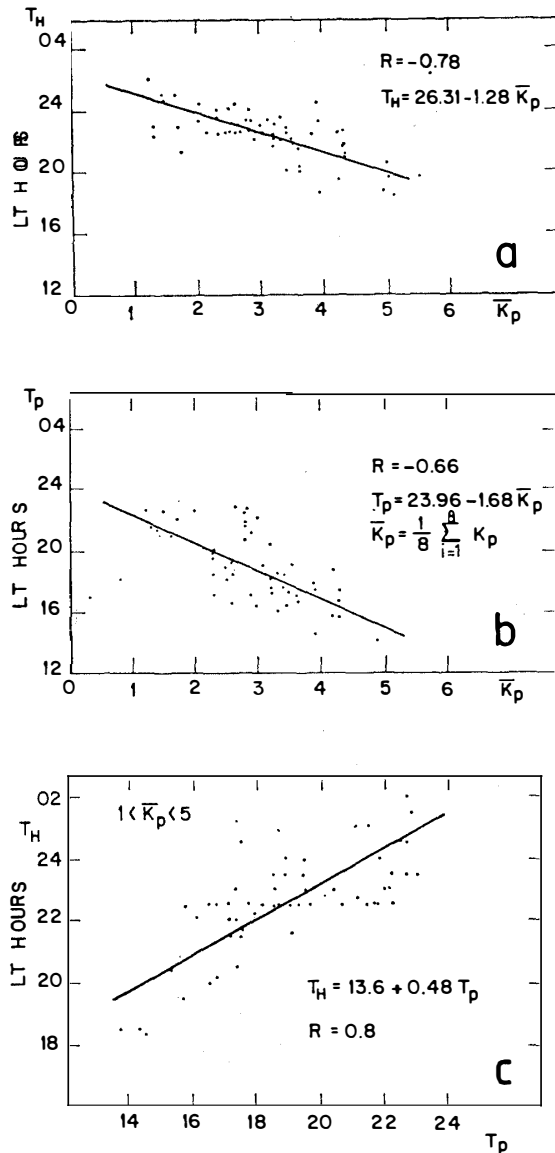spheric electric field when the magnetic activity increases (Fig. 19).

Fig. 18. Local time values of the Harang discontinuity, T_H and of the eastward border of the plasmasphere boundary, T_P. (a) Statistical relation between T_H and Kp. (b) Statistical relation between T_P and Kp. (c) Case by case comparison between T_H and T_P. Here $\overline{Kp}$ is the 24 h average value of the planetary geomagnetic index Kp (after Zi et al., 1982).
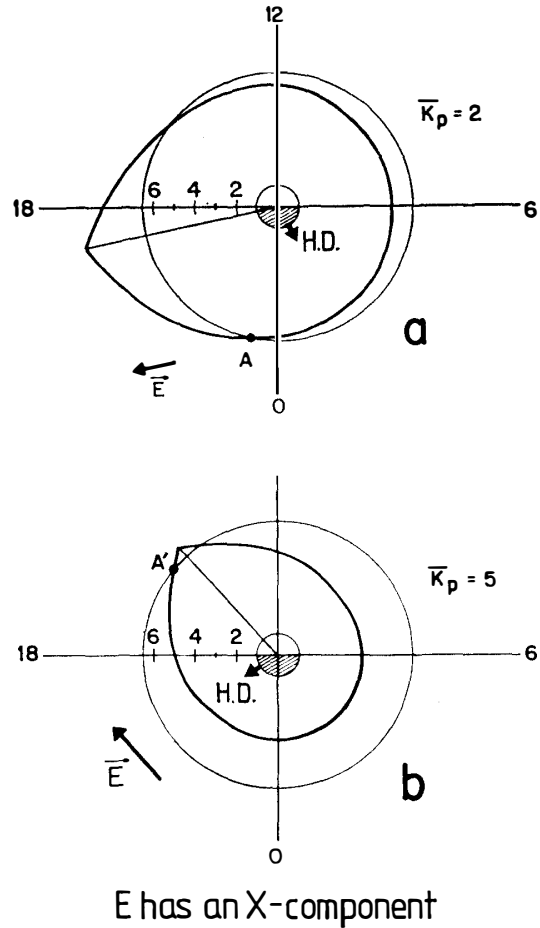
Fig. 19. A possible interpretation of the variation of T_H and T_P with Kp. The local times of both the Harang discontinuity and the eastward boundary of the plasmaspheric bulge as encountered by GEOS-2 are linked with the direction of the magnetospheric electric field E, which has a stronger X-component when Kp increases. But when Kp increases, $|E|$ also increases and the plasmasphere shrinks, so that the variation of T_P is larger than that of T_H (after Zi et al., 1982).

4.3. Equatorial and ionospheric signatures of global convection

EISCAT being located near the foot print of the GEOS-2 field line, it was tempting to compare the results obtained with the two facilities, as far as the convection and corotation magnetospheric plasma processes are concerned. This has been done for a few events when both EISCAT and GEOS-2 were operating in the convenient
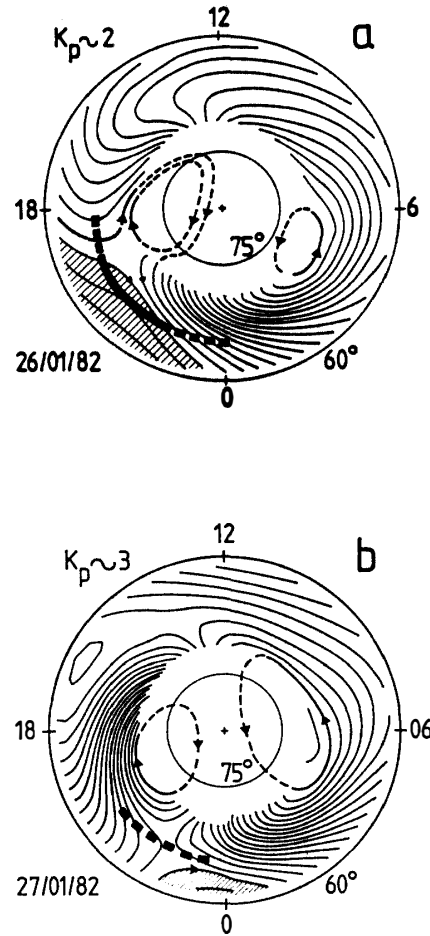
Fig. 20.   Comparative analysis of GEOS and EIS-CAT data related with the global magnetospheric convection.   Auroral equipotential lines as deduced from 24 h EISCAT data are plotted (2 kV between lines for a, 4 kV for b.)   The trace of the GEOS foot print in this local time presentation is also plotted as a thick line, continuous when GEOS observations indicate the presence of a high plasma density, discontinuous when GEOS was not within the plasmasphere.   The plasma-pause boundary coincides with the first corotation equipotential (after FONTAINE et al., 1986b).

modes.   Maps of ionospheric potentials, for geomagnetic latitudes ranging between 62° and 72° have been drawn by processing data obtained with EISCAT over 24 h periods.   Examples of such maps are presented on Fig. 20 (FONTAINE et al., 1986b). They show the classical two-cells convection pattern over the polar cap which can be distinguished from the circular corotation pattern which prevails at lower latitudes. Superimposed one these maps, the trace of the GEOS-2 foot print is also drawn in such a local time representation.   The continuous line corresponds to local times during which GEOS-2 was situated within the plasmaspheric bulge, as determined by the high value of the plasma density.   One sees that the bulge position corresponds to regions where corotation dominates (Fig. 20a).   On the contrary, in another situation (Fig. 20b) GEOS-2 did not encounter the plasmaspheric bulge and its foot print was situated in the convection-dominated region, as determined from the analysis of EIS-CAT data.   These results demonstrate that the whole plasmasphere, from the equatorial plane down to ionospheric altitudes, corotates with the Earth.

5.   Short Irregular Pulsations (SIP) and Field-Aligned Current Structures

The last phenomenon which will be described is related to the observation, made with the GEOS ULF magnetic sensors, of what is usually called Short Irregular Pulsa-

tions or SIP's (see Fig. 3c), Such a phenomenon has been interpreted in terms of intense, space-limited field-aligned currents (ROBERT *et al.*, 1984). Though important are the geophysical implications of such an interpretation this discovery does not seem to have yet received the attention it deserves.

5.1. SIP's: a substorm-related phenomenon

During the GEOS-2 lifetime a lot of GBR experiments have been planned and performed in order to study the spatial and temporal variation of auroral phenomena along a specific meridian. Among these experiments, optical observations have allowed to study the development of auroral forms during magnetospheric substorms. An example of such observations is given on Fig. 21. The bottom pannel shows the variation of the auroral luminosity as detected by a 630 nm zenithal photometer situated at Kilpisjärvi, Finland. One notices the abrupt increase of the auroral luminosity which is associated with the northward displacement of auroral forms during break-ups, as evidenced by the examination of all sky camera images (SHEPHERD *et al.*, 1980).

The top pannel, which deals with particle fluxes detected onboard GEOS, shows the pre-substorm depletion associated with the stretching of magnetic field-lines, and
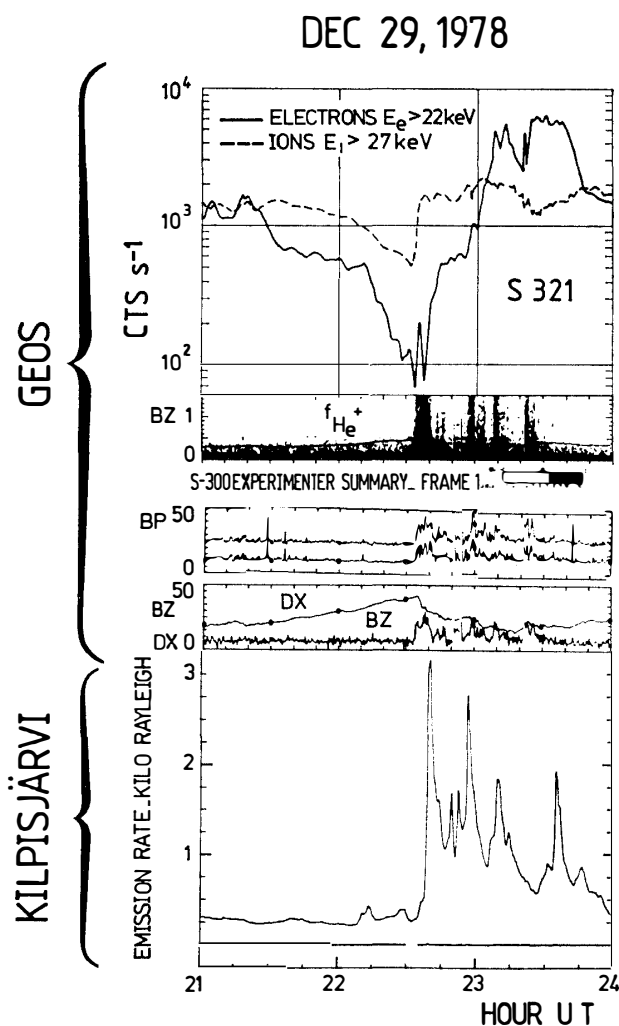

Fig. 21. Ground and satellite measurements before and during auroral break up. Upper pannel (No. 1): electrons and ions fluxes (GEOS). Pannel No. 2: Spectrogram of ULF waves between 0 and 1.5 Hz (GEOS). Pannel No. 3: ULF wave intensity between 1.5 and 5 Hz and between 5 and 11 Hz (GEOS). Pannel No. 4: ULF wave intensity between 0.3 and 1.5 Hz (lower curve) and DC magnetic field intensity in the plane perpendicular to the Earth's axis (higher curve) (GEOS). Pannel No. 5: auroral luminosity around 630 nm (Kilpisjärvi) (SHEPHERD et al., 1980).

the subsequent particle injection. The fourth pannel from the top shows the pre-substorm increase of the DC magnetic component situated in the Earth equatorial plane, denoted by DX. Such a progressive increase of DX is associated with the inward displacement of the tail neutral sheet current. This increase is followed by an abrupt decrease (around 2234 UT) which corresponds to a return of magnetic field lines toward their dipolar-like structure. At this very time, which is associated with the abrupt increase of auroral luminosity above Kilpisjärvi, one notices the appearance of strong impulsive ULF turbulance, as evidenced on the spectrogram (second pannel from the top) or by the amplitude-versus-time curves (third and fourth pannel). The analysis of similar events has shown that SIP's occur at time of magnetospheric
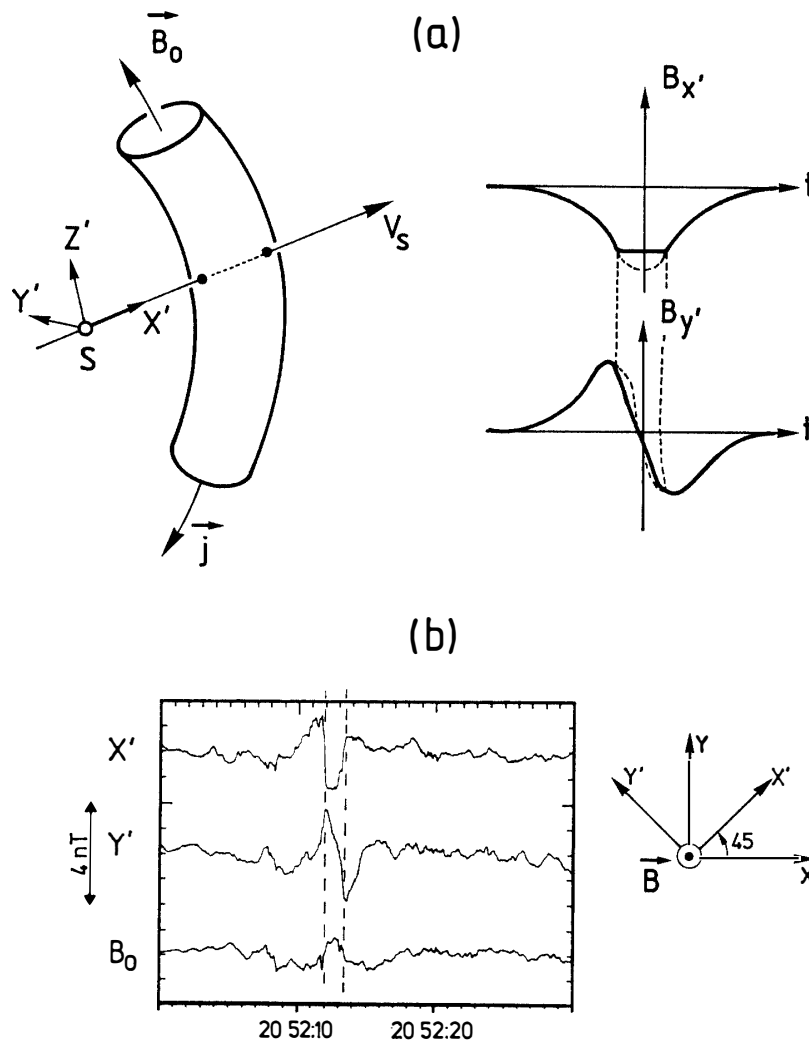

Fig. 22. Magnetic signature of a moving small-scale FAC observed onboard GEOS-2 on February 15, 1980. (a) Assuming that the spacecraft is moving through the structure with a velocity v_s (instead of the structure passing by the spacecraft with a velocity $-v_s$), one gets the theoretical signatures represented on the right. (b) In reality, the antennas XYZ do not have the simple orientation $X'Y'Z'$; but by a rotation of the axis, one gets signatures which ressemble the theoretical ones (ROBERT et al., 1984).

substorms, as detected both by particle and DC magnetic field sensors onboard GEOS and by photometers placed in the conjugate area.

5.2. SIP'S: signature of intense field-aligned current (FAC) structures

In an attempt to construct the 3-D hodograms of the magnetic vector associated with SIP's, Robert et al. (1984) discovered that such signals in fact could be interpreted as the signature of rapidly moving field-aligned current structures, whose transverse dimensions would be of the order of a few proton gyroradii (i.e. a few hundreds of kilometers). Figure 22 shows both the magnetic signal that one could expect from such moving structures and an example of their magnetic signature.

Table 2. Small-scale field-aligned current characteristics. Equatorial values are deduced from magnetic and electric measurement onboard GEOS-2. Ionospheric values are deduced from the previous ones, assuming current conservation within flux tubes (Robert et al., 1984).

	Minimum	Maximum	Average
Equatorial values			
Radius R_e, km	20	900	215
Current density J_e, $\mu A \cdot m^{-2}$	6×10^{-3}	0. 3	8×10^{-2}
Velocity v_e, km/s	15	170	70
Ionospheric values			
Radius R_i, km	1	40	10
Current density J_i, $\mu A \cdot m^{-2}$	3	150	40
Velocity v_i, km/s	1	10	4. 5

By combining these magnetic measurements with simultaneous electric field data, it has been possible to deduce the characteristic parameters (radius, current density, displacement velocity) of some 28 events. The average, minimum and maximum values of these parameters are reported in Table 2. Such intense and rapidly moving currents could be the manifestation of a disruption in the neutral sheet current, since they are associated with a return of the geomagnetic field toward a dipolar configuration.

5.3. Ionospheric evidence of small scale FAC's

On the basis of these results, Robert et al. (1984) made an evaluation of the characteristics that such structures should have at ionospheric altitudes if the current were transmitted by conserving the geometry of the flux tubes (second part of Table 2). The current density of these structures would be much larger ($\sim$100 $\mu A \cdot m^{-2}$) than that of the large scale FAC structures reported by Iijima and Potemra (1978), which is of the order of a few $\mu A \cdot m^{-2}$.

It is interesting to note that some ten years ago, similar short scale FAC's were assumed in order to interpret AC magnetic signals detected onboard OGO 4 (Berko et al., 1975). Recent measurements onboard ARCAD-3 have proven that such intense ($\sim$100 $\mu A \cdot m^{-2}$) and localized (R $\sim$0.1 km) currents indeed existed at ionospheric altitudes (Machard et al., 1985). Two example of such structures are represented on Fig. 23. In that case, the alternative nature of the signal is not due to the displacement of the current but to that of the spacecraft which moves at a velocity of about 8
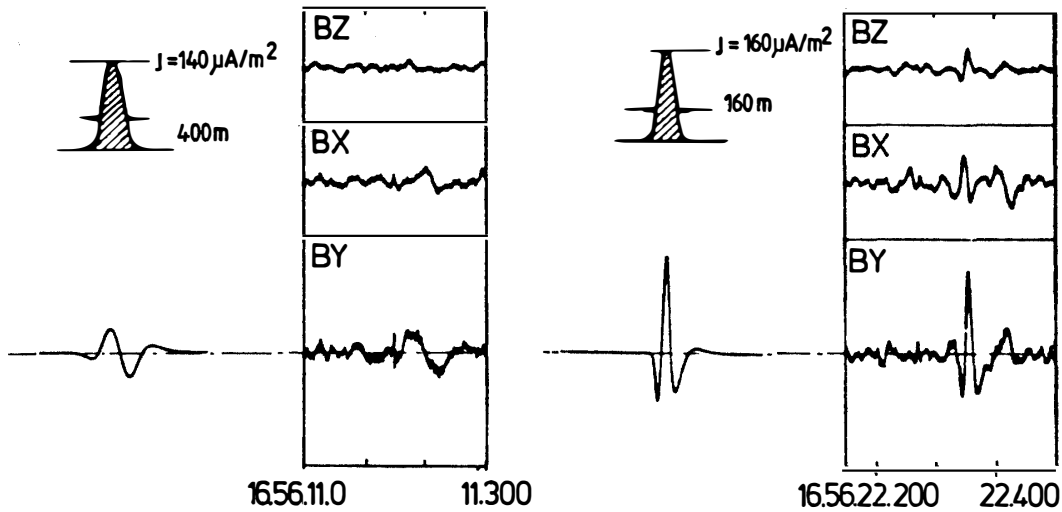
Fig. 23. Two small-scale field-aligned currents detected at ionospheric altitudes onboard ARCAD-3 (June 26, 1982). For each event the signal is represented on the right and the model on the left (after MACHARD et al., 1985).

km/s in the vicinity of the structure. However, it seems that these signatures could as well be interpreted in terms of LF turbulence whereas FAC's with larger size (~1–2 km) have been identified onboard the same spacecraft, their characteristics being more in agreement with the predictions deduced from the GEOS-2 measurements (A. BERTHELIER, private communication, 1987).

The size of such structures is too small to allow their simultaneous measurement at the apex of the field line and at its footprint. But the existence of localized currents is apparently a common phenomenon since they seem to have been observed in the tail lobes (LI et al., 1986). As suggested many times by Alfvén, filamentary structures are a characteristic of cosmical plasmas, and their identification in the accessible magnetosphere is of utmost interest.

6. Conclusions

Observations made with the European spacecraft GEOS in conjunction with associated GBR experiments have been very productive. They have allowed to distinguish processes which can be observed only at the apex of the field line from those which can be also detected at ground. They have helped to clarify the conditions of generation of some electromagnetic waves, the relationships between magnetospheric and ionospheric convection, and the nature of some substorm processes. The use of GEOS alone has been at the origin of the discovery of the role of heavy ions in ICW's generation, of the existence of an important non-dawn-to-dusk electric field component, and of the presence of intense small-scale FAC's in the equatorial region during substorms.

There is still a lot of problems which could be elucidated by doing simultaneous measurements at the apex of field lines and at their foot prints. Unfortunately it is doubtful that there will be, in any expectable future, another geostationary satellite purely devoted to scientific magnetospheric research. However the possibility of

allocating a small fraction of weight, bit rate and power to scientific equipments devoted to well-specified research onboard future application satellites should be favorably considered by Space Agencies.

Besides, one must not forget that the research which was done with GEOS and other equatorial satellites, in conjunction with ground observations was mainly devoted to mid-latitude and auroral phenomena. Future scientific projects could be concentrated on the study of polar cap phenomena in both hemispheres. These regions are more loosely connected via geomagnetic field lines than mid-latitude or auroral regions. On the other hand they are linked together through interplanetary magnetic field lines. The simultaneous study of polar cap processes by means of two spacecraft in opposite hemispheres and in conjunction with associated ground campaigns could well be the starting point of new discoveries to be made in the study of magnetic conjugacy.

Acknowledgments

References

ASHOUR-ABDALLA, M. and KENNEL, C. F. (1978): Diffuse auroral precipitation. J. Geomagn. Geoelectr., 30, 239–255.

BELMONT, G., FONTAINE, D. and CANU, P. (1983): Are equatorial electron waves responsible for diffuse auroral electron precipitation? J. Geophys. Res., 88, 9163–9170.

BELMONT, G., FONTAINE, D. and CANU, P. (1984): Reply. J. Geophys. Res., 89, 7591–7592.

BERCHEM, J. and GENDRIN, R. (1985): Nonresonant interaction of heavy ions with electromagnetic ion cyclotron waves. J. Geophys. Res., 90, 10945–10960.

BERKO, F. W., HOFFMANN, R. A., BURTON, R. K. and HOLZER, R. E. (1975): Simultaneous particle and field observations of field-aligned currents. J. Geophys. Res., 80, 37–46.

BRICE, N. M. (1965): Multiphase period very low frequency emission. Radio Sci., **69D**, 257–265.

CANU, P. (1982): Etude expérimentale des ondes électrostatiques électroniques détectées dans la magnétosphère terrestre par le satellite GEOS-2. Thesis, Université Paris-6.

CHEN, A. J. and WOLF, R. A. (1972): Effects on the plasmasphere of a time varying convection electric field. Planet. Space Sci., **20**, 483–509.

CHRISTIANSEN, P. J., GOUGH, M. P. and RONMARK, K. (1980): Electron cyclotron waves in the Earth's magnetosphere. Exploration of the Polar Upper Atmosphere, ed. by C. S. DEEHR and J. A. HOLTET. Dordrecht, D. Reidel, 355–366.

CORNILLEAU-WEHRLIN, N. (1981): A new ULF-modulated electrostatic wave detected in the extremely low frequency range onboard GEOS. J. Geophys. Res., **86**, 1365–1373.

CORNILLEAU-WEHRLIN, N., GENDRIN, R., LEFEUVRE, F., PARROT, M., GRARD, R., JONES, D., BAHNSEN, A., UNGSTRUP, E. and GIBBONS, W. (1978a): VLF electromagnetic waves observed onboard GEOS-1. Space Sci. Rev., **22**, 371–382.

CORNILLEAU-WEHRLIN, N., GENDRIN, R. and TIXIER, M. (1978b): VLF waves; Conjugated ground-satellite relationships. Space Sci. Rev., **22**, 419–431.

CORNILLEAU-WEHRLIN, N., GENDRIN, R. and PEREZ, R. (1978c): Reception of the NKL (Jim Creek) transmitter onboard GEOS-1. Space Sci. Rev., **22**, 433–442.

CORNILLEAU-WEHRLIN, N., SOLOMON, J., KORTH, A. and KREMSER, G. (1985): Experimental study of the relationship between energetic electrons and ELF waves observed onboard GEOS; A support to quasi-linear theory. J. Geophys. Res., **90**, 4141–4154.

CORONITI, F. V. and KENNEL, C. F. (1970): Electron precipitation pulsations. J. Geophys. Res., **75**, 1279–1289.

DECREAU, P. M. E., BEGHIN, C. and PARROT, M. (1978a): Electron density and temperature, as measured by the mutual impedance experiment onboard GEOS-1. Space Sci. Rev., **22**, 581–595.

DECREAU, P. M. E., ETCHETO, J., KNOTT, K., PEDERSEN, A., WRENN, G. L. and YOUNG, D. T. (1978b): Multi-experiment determination of plasma density and temperature. Space Sci. Rev., **22**, 633–645.

ETCHETO, J. and BLOCH, J. J. (1978): Plasma density measurements from the GEOS-1 relaxation sounder. Space Sci. Rev., **22**, 597–610.

ETCHETO, J., GENDRIN, R., SOLOMON, J. and ROUX, A. (1973): A self-consistent theory of magnetospheric ELF hiss. J. Geophys. Res., **78**, 8150–8166.

FONTAINE, D., PERRAUT, S., CORNILLEAU-WEHRLIN, N., APARICIO, B., BOSQUED, J. M. and RODGERS, D. (1986a): Coordinated observations of electron energy spectra and electrostatic waves during diffuse auroras. Ann. Geophys., **4**, 405–412.

FONTAINE, D., PERRAUT, S., ALCAYDE, D., CAUDAL, G. and HIGEL, B. (1986b): Large scale structures of the convection inferred from coordinated measurements by EISCAT and GEOS-2. J. Atmos. Terr. Phys., **48**, 973–986.

GENDRIN, R. (1970): Substorm aspects of magnetic pulsations. Space Sci. Rev., **11**, 54–130.

GENDRIN, R. (1981): General relationships between wave amplification and particle diffusion in a magnetoplasma. Rev. Geophys. Space Phys., **19**, 171–184.

GENDRIN, R. (1983): Wave-particle interactions as an energy transfer mechanism between different particle species. Space Sci. Rev., **34**, 271–287.

GENDRIN, R. and ROUX, A. (1980): Energization of helium ions by proton-induced hydromagnetic waves. J. Geophys. Res., **85**, 4577–4586.

GENDRIN, R., PERRAUT, S., FARGETTON, H., GLANGEAUD, F. and LACOUME, J. L. (1978): ULF waves; Conjugated ground-satellite relationships. Space Sci. Rev., **22**, 433–442.

GENDRIN, R., ASHOUR-ABDALLA, M., OMURA, Y. and QUEST, K. (1984): Linear analysis of ion cyclotron interaction in a multicomponent plasma. J. Geophys. Res., **89**, 9119–9124.

GOUGH, M. P., CHRISTIANSEN, P. J. and GERSHUNY, E. (1981): E.S. wave morphology near the geostationary orbit. Adv. Space Res., **1**, 337–343.

GREENWALD, R. A., WEISS, W., NIELSEN, E. and THOMSON, N.R. (1978): STARE; A new radar auroral backscatter experiment in northern Scandinavia. Radio Sci., **13**, 1021–1039.

HELLIWELL, R. A. (1963): Whistler-triggered VLF emissions. J. Geophys. Res., **68**, 5387–5395.

HIGEL, B. (1978): Small scale structure of magnetospheric electron density through online tracking of plasma resonances. Space Sci. Rev., **22**, 611–631.

HIGEL, B. and WU, L. (1984): Electron density and plasmapause characteristics at 6.6 R_E; A statistical study of the GEOS-2 relaxation sounder data. J. Geophys. Res., **89**, 1583–1601.

HUGHES, W. J. and GRARD, R. J. L. (1984): A second harmonic geomagnetic field line resonance at the inner edge of the plasma sheet; GEOS-1, ISEE-1, and ISEE-2 observations. J. Geophys. Res., **89**, 2755–2764.

HUGHES, W. J. and SOUTHWOOD, D. J. (1976): The screening of micropulsation signals by the atmosphere and ionosphere. J. Geophys. Res., **81**, 3234–3240.

IIJIMA, T. and POTEMRA, T. A. (1978): Large-scale characteristics of field-aligned currents associated with substorms. J. Geophys. Res., **83**, 599–615.

INHESTER, B., WEDEKEN, U., KORTH, A., PERRAUT, S. and STOKHOLM, M. (1984): Ground-satellite coordinated study of the April 5, 1979 events; Observation of O^+ cyclotron waves. J. Geophys., **55**, 134–141.

JONES, D. (1978): Introduction to the S-300 wave experiment onboard GEOS. Space Sci. Rev., **22**, 327–332.

JUNGINGER, H., BAUER, O. H., HAERENDEL, G., MELZNER, F., HIGEL, B. and AMATA, E. (1983): Plasma drift measurements with the electron beam experiment on GEOS-2 during long period pulsations on April 7, 1979. Geophys. Res. Lett., **10**, 667–670.

JUNGINGER, H., GEIGER, G., HAERENDEL, L. G., MELZNER, F., AMATA, E. and HIGEL, B. (1984): A statistical study of dayside magnetospheric electric field fluctuations with periods between 150 and 600 s. J. Geophys. Res., **89**, 5495–5505.

KENNEL, C. F. and PETSCHEK, H. E. (1966): Limit on stably particle fluxes. J. Geophys. Res., **71**, 1–28.

KENNEL, C. F., SCARF, F. L., FREDRICKS, R. W., McGEHEE, J. H. and CORONITI, F. V. (1970): VLF electric field observations in the magnetosphere. J. Geophys. Res., **75**, 6136–6152.

KIMURA, I. (1974): Interrelation between VLF and ULF emissions. Space Sci. Rev., **16**, 389–411.

KITAMURA, T., JACOBS, J. A., WATANABE, T. and FLINT, R. B. (1969): An investigation of quasi-periodic VLF emissions. J. Geophys. Res., **74**, 5652–5664.

KNOTT, K. (1975): Payload of the GEOS scientific geostationary satellite. ESA/ASE Sci. Tech. Rev., **1**, 173–196.

KNOTT, K., DURNEY, A. and OGILVIE, K., ed. (1979): Advances in Magnetospheric Physics with GEOS-1 and ISEE. Dordrecht, D. Reidel, 627p.

KORTH, A., KREMSER, G., ROUX, A., PERRAUT, S., SAUVAUD, J.A., BOSQUED, J. M., PEDERSEN, A. and APARICIO, B. (1983): Drift boundaries and ULF wave generation near noon at geostationary orbit. Geophys. Res. Lett., **10**, 639–642.

KREMSER, G., KORTH, A., FEJER, J. A., WILKEN, B., GUREVITCH, A. V. and AMATA, E. (1981): Observations of quasi-periodic flux variations of energetic ions and electrons associated with Pc5 geomagnetic pulsations. J. Geophys. Res., **86**, 3345–3356.

KREMSER, G., KORTH, A., ULLALAND, S., STADSNES, J., BAUMJOHANN, W., BLOCK, L., TORKAR, K. M., RIEDLER, W., APARICIO, B., TANSKANEN, P., IVERSEN, I. B., CORNILLEAU-WEHRLIN, N., SOLOMON, J. and AMATA, E. (1986): Energetic electron precipitation during a magnetospheric substorm and its relationship to wave particle interaction. J. Geophys. Res., **91**, 5711–5718.

KÜPPERS, F., UNTIEDT, J., BAUMJOHANN, W., LANGE, K. and JONES, A. G. (1979): A two-dimensional magnetometer array for ground-based observations of auroral zone electric currents during the International Magnetospheric Study (IMS). J. Geophys., **46**, 429–459.

LI, Y., XU, R. L. and FAN, C. Y. (1986): Particle bursts and filamentary current in the magnetotail lobe observed by ISEE-1. Proceedings of the International Symposium on Space Physics, ed. by Chinese Society of Space Research and Chinese Academy of Sciences, Beijing, 4.063–4.066.

LYONS, L. R. (1974): Electron diffusion driven by magnetospheric electrostatic waves. J. Geophys. Res., **79**, 575–580.

MACHARD, C., BERTHELIER, A., BERTHELIER, J. J., CERISIER, J. C., GALPERIN, Y. I. and MOGILEVSKY, M. M. (1985): Small scale and intense field-aligned currents detected by their magnetic signature. Results of the ARCAD-3 Project and of the Recent Programmes in Magnetospheric and Ionospheric Physics, Toulouse, CEPADUES-Editions, 93–97.

NEUBERT, T., LEFEUBRE, F., PARROT, M. and CORNILLEAU-WEHRLIN, N. (1983): Observations on GEOS-1 of whistler mode turbulence generated by a ground-based VLF transmitter. Geophys. Res. Lett., 10, 623–626.

NIELSEN, E. and GREENWALD, R. A. (1979): Electron flow and visual aurora at the Harang discontinuity. J. Geophys. Res., 84, 4189–4200.

NORRIS, A. J., JOHNSON, J. F., SOJKA, J. J., WRENN, G. L., CORNILLEAU-WEHRLIN, N., PERRAUT, S. and ROUX, A. (1983): Experimental evidence for the acceleration of thermal electrons by ion cyclotron waves in the magnetosphere. J. Geophys. Res., 88, 889–898.

OMURA, Y., ASHOUR-ABDALLA, M., GENDRIN, R. and QUEST, K. (1985): Heating of thermal helium in the equatorial magnetosphere; A simulation study. J. Geophys. Res., 90, 8281–8292.

PERRAUT, S., GENDRIN, R., ROBERT, P., ROUX, A., DE VILLEDARY, C. and JONES, D. (1978): ULF waves observed with magnetic and electric sensors on GEOS-1. Space Sci. Rev., 22, 347–369.

PERRAUT, S., ROUX, A., ROBERT, P., GENDRIN, R., SAUVAUD, J. A., BOSQUED, J. M., KREMSER, G. and KORTH, A. (1982): A systematic study of ULF waves above F_{H^+} from GEOS 1 and 2 measurements and their relationships with proton ring distributions. J. Geophys. Res., 87, 6219–6236.

PERRAUT, S., GENDRIN, R., ROUX, A. and DE VILLEDARY, C. (1984): Ion cyclotron waves; Direct comparison between ground-based measurements and observations in the source region. J. Geophys. Res., 89, 195–202.

RAUCH, J. L. and ROUX, A. (1982): Ray tracing of ULF waves in a multicomponent plasma; Consequences for the generation mechanisms of ion cyclotron waves. J. Geophys. Res., 87, 8191–8198.

ROBERT, P., GENDRIN, R., PERRAUT, S. and ROUX, A. (1984): GEOS 2 identification of rapidly moving current structures in the equatorial outer magnetosphere during substorms. J. Geophys. Res., 89, 819–840.

ROUX, A., PERRAUT, S., RAUCH, J. L., DE VILLEDARY, C., KREMSER, G., KORTH, A. and YOUNG, D. T. (1982): Wave-particle interactions near Ω_{He^+} observed on board GEOS 1 and 2: 2. Generation of ion cyclotron waves and heating of He^+ ions. J. Geophys. Res., 87, 8174–8190.

ROUX, A., CORNILLEAU-WEHRLIN, N. and RAUCH, J. L. (1984): Acceleration of thermal electrons by ICW's propagating in a multicomponent magnetospheric plasma. J. Geophys. Res., 89, 2267–2273.

S-300 EXPERIMENTERS (1979): Measurements of electric and magnetic wave fields and of cold plasma parameters onboard GEOS-1; Preliminary results. Planet Space Sci., 27, 317–339.

SATO, N. and FUKUNISHI, H. (1981): Interaction between ELF-VLF emissions and magnetic pulsations; Classification of quasi-periodic ELF-VLF emissions based on frequency-time spectra. J. Geophys. Res., 86, 9–18.

SATO, N. and KOKUBUN, S. (1980): Interaction between ELF-VLF emissions and magnetic pulsations; Quasi-periodic ELF-VLF emissions associated with Pc 3-4 magnetic pulsations and their magnetic conjugacy. J. Geophys. Res., 85, 101–113.

SATO, N. and KOKUBUN, S. (1981): Interaction between ELF-VLF emissions and magnetic pulsations; Regular period ELF-VLF pulsations and their geomagnetic conjugacy. J. Geophys. Res., 86, 9–18.

SHEPHERD, G. G., BOSTRÖM, R., DERBLOM, H., FÄLTHAMMAR, C. G., GENDRIN, R., KAILA, K., KORTH, A., PEDERSEN, A., PELLINEN, R. and WRENN, G. L. (1980): Plasma and field signatures of propagating impulsive precipitation observations at the foot of the GEOS-2 field line. J. Geophys. Res., 85, 4587–4601.

SONG, X. T. and CAUDAL, G. (1987): Electron density near the plasmapause measured over one year by GEOS-2; A statistical analysis. J. Atmos. Terr. Phys., 49, 135–144.

SONG, X. T., GENDRIN, R., CAUDAL, G. and BLANC, M. (1987a): Refilling process of the plasmasphere and its relation to magnetic activity. to be published in J. Atmos. Terr. Phys.

Song, X. T., Gendrin, R. and Blanc, M. (1987b): Determination of the Volland convection electric field parameters and computation of the associated field-aligned currents distribution. submitted to Planet. Space Sci.

Takahashi, K. and McPherron, R. L. (1982): Harmonic structure of Pc 3–4 pulsations. J. Geophys. Res., **87**, 1504–1516.

Tixier, M. and Cornilleau-Wehrlin, N. (1986): How are the VLF quasi-periodic emissions controlled by harmonics of field line oscillations? The results of a comparison between ground and GEOS satellites measurements. J. Geophys. Res., **91**, 6899–6919.

Tonegawa, Y., Fukunishi, H., Hirasawa, T., McPherron, R. L., Sakurai, T. and Kato, Y. (1984): Spectral characteristics of Pc 3 and Pc 4/5 magnetic pulsation bands observed near $L=6$. J. Geophys. Res., **89**, 9720–9730.

Ungstrup, E., Neubert, T. and Bahnsen, A. (1978): Observations on GEOS-1 of 10.2 to 13.6 kHz ground based transmitter signals. Spece Sci. Rev., **22**, 453–464.

Walker, A. D. M., Greenwald, R. A., Korth, A. and Kremser, G. (1982): STARE and GEOS-2 observations of a storm time Pc 5 ULF pulsation. J. Geophys. Res., **87**, 9135–9146.

Wedeken, U., Inhester, B., Korth, A., Glassmeier, K.-H., Gendrin, R., Lanzerotti, L. J., Gough, H., Green, C. A., Amata, E., Pedersen, A. and Rostoker, G. (1984): Ground-satellite coordinated study of the April 5, 1979 events; Flux variations of energetic particles and associated magnetic pulsations. J. Geophys., **55**, 120–133.

Wu, L., Gendrin, R., Higel, B. and Berchem, J. (1981): Relationships between the solar wind electric field and the magnetospheric convection electric field. Geophys. Res. Lett., **8**, 1099–1102.

Wu, L., Song, X. T. and Barouch, E. L. (1985): Experimental parameters for the Volland convection electric field model. Chinese J. Space Sci., **5**, 25–32.

Yamagishi, H., Fukunishi, H., Kojima, T., Yoshino, T. and Gendrin, R., (1984): Conjugate observation of periodic VLF emissions near $L=6$. Mem. Natl Inst. Polar Res., Spec. Issue, **31**, 94–114.

Young, D. T., Perraut, S., Roux, A., De Villedary, C., Gendrin, R., Korth, A., Kremser, G. and Jones, D. (1981): Wave-particle interactions near Ω_{He^+} observed on GEOS 1 and 2; 1. Propagation of ion cyclotron waves in He^+-rich plasma. J. Geophys. Res., **86**, 6755–6772.

Zi, M.-Y., Wu, L., Gendrin, R. and Higel, B. (1982): The Harang discontinuity and the evening plasmapause boundary; A STARE-GEOS intercomparison. J. Atmos. Terr. Phys., **44**, 671–679.